Research article

Plasma-induced nanostructured metallic silver surfaces: study of bacteriophobic effect to avoid bacterial adhesion on medical devices
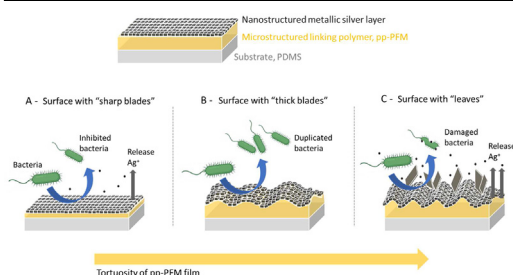
Cristina García-Bonillo [a,b], Robert Texidó [a], Joan Gilabert-Porres [b], Salvador Borrós [a,b,*]

[a] *Grup d'Enginyeria de Materials (GEMAT), Universitat Ramón Llull, 08017, Barcelona, Spain*
[b] *Tractivus SL, 08017, Barcelona, Spain*

GRAPHICAL ABSTRACT

ARTICLE INFO

ABSTRACT

Biofilm formation in medical devices represents one of the major problems for the healthcare system, especially those that occur on implantable silicone-based devices. To provide a general solution to avoid biofilm formation in the first stages of development, this work studied how nanostructured metallic silver coatings hinder bacteria-surface interaction by preventing bacteria adhesion. The three studied silver nanostructures ("Sharp blades", "Thick blades" and "Leaves") combined superhydrophobic behavior with a physical impediment of the coating nanostructure that produced a bacteriophobic effect avoiding the adhesion mechanism of different bacterial strains. These silver nanostructures are immobilized on stretchable substrates through a polymeric thin film of plasma–polymerized penta-fluorophenyl methacrylate. The control over the nanostructures and therefore its bacteriophobic—bactericidal effect depends on the plasma polymerization conditions of the polymer. The characterization of this bacteriophobic effect through FE-SEM microscopy, live/dead cell staining, and direct bacterial adhesion counts, provided a complete mapping of how bacteria interact with the surface in each scenario. Results revealed that the bacterial adhesion was reduced by up to six orders of magnitude in comparison with uncoated surfaces thereby constituting an effective strategy to avoid the formation of biofilm on medical materials.

1. Introduction

Health care-associated infections (HCAIs) are those infections that patients acquire while receiving health care [1, 2]. Usually, HCAIs appear after 48 h of hospitalization and last between 7 and 20 days, with the risk of becoming chronic [2, 3]. These infections are associated with the implantation of a medical device in more than 80% of cases [2, 4, 5].

Bacterial colonization onto medical devices can originate from multiple bacterial species, but the colonization onto the surface of a medical device has a common adhesion mechanism [6, 7]. Briefly, bacteria

* Corresponding author.
E-mail address: salvador.borros@iqs.url.edu (S. Borrós).

interact with the surface of the device and adhere to it by their appendages or adhesion systems. The bacteria then excrete extracellular matrix creating a consolidated structure that matures as a biofilm [6, 8, 9, 10, 11]. Besides these complications, bacteria develop a high resistance to antibiotics and biocides commonly used in hospitals [12, 13] and have even incorporated genetic elements of resistance to antibiotics that confer them the ability to survive prolonged treatments [14, 15].

In this scenario, bacterial evolution has cast doubts on the well-established therapies creating a new medical paradigm for a post-antibiotic era [12], with no antibiotics (or restricted use). The main approaches are focused on the modification of the medical device surface to provide antibacterial properties [16] through the immobilization of bactericide agents allowing their release. Most common strategies involve bactericide agents, such as metallic ions of silver [17], copper [18], zinc [19] and chloride or iodine salts [20]. Among them, metallic ions are generating special attention due to the fact that they can simultaneously produce a bacterial wall disruption as well as reactive oxygen species; two mechanisms for killing bacteria, against which it is really difficult to develop resistance [21, 22]. The release of metallic ions from the surface of a medical device ensures high mortality rates of bacteria in the first hours of implantation [23, 24]. However, a sustained release of metal ions from a coating is very difficult to achieve and when the bactericide agent is exhausted the devices remain completely unprotected against bacteria [10, 25, 26]. To provide a solution to overcome these limitations, a new approach based on surface topography is attracting interest. Bacterial colonization is avoided through the utilization of surfaces with poor interaction with bacteria [27]. In this context, the use of micro and nanopatterns, self-cleaning and low adhesion surfaces have shown interesting results in modulating bacterial growth and adhesion mechanism once in contact with the surfaces [28]. The ideal bacteriophobic surface must also be super-hydrophobic since, although the surface has antimicrobial elements such as metals, it is interesting not to favor bacterial adhesion to these elements. If bacteria adhere to the antimicrobial coating, even if they die, a layer of dead biological matter is created on the coating that hinders the release of antimicrobial agents. This layer causes the bactericidal effect to be lost in a short period of time. The prevention of bacterial adhesion is achieved by creating a bacteriophobic micro- and nanostructure with the possibility of incorporating a bactericidal or bacteriostatic environment through the controlled release of antimicrobial substances. These strategies are now being considered for the next generation of antimicrobial surfaces [28, 29, 30] due to the fact that 1) the bacteriophobic mechanism is based on physical impediments and lower interactions that limit bacteria attachment in the first stages of biofilm formation [31]; and 2) the release of silver ions interferes with bacterial growth and their proliferation in a controlled manner near the surface. These synergic mechanisms are a promising strategy for avoiding bacterial adhesion in terms of effectiveness, long duration and, even more importantly, because they are common to a wide range of bacterial strains.

This work studied how morphological changes in the micro and nano structure of a surface can lead to significant differences in bacterial adhesion. Specifically, plasma polymerized penta-fluorophenyl methacrylate (pp-PFM) thin films deposited on stretchable substrates (such as silicone) were used to immobilize a continuous layer of metallic silver via Tollens' reaction. Through plasma polymerization conditions, PFM film roughness and thickness was controlled thereby modifying the micro and nano structure of the metallic silver layer. Three main surface morphologies were identified through field emission microscopy (FE-SEM) and to understand how biological media interacts with these surfaces and discuss the requirements for an eventual "bacteriophobic effect" their wettability (WCA), their silver content (ICP), was studied together with their ability to adsorb proteins (micro-BCA). Bacterial adhesion and the bacteriophobic effect of each surface was studied using different bacterial strains (gram-negative *Pseudomonas aeruginosa* and *E. coli*, and gram-positive *S. aureus*). A different characterization technique was also used to study the relationship between bacteria and surfaces. FE-SEM revealed how bacteria was immobilized on each surface proving an insight into the mechanism of bacteria adhesion. Confocal microscopy allowed differentiation between live and dead bacteria in the surface surroundings, establishing whether the surface effect was bacteriophobic or bactericide. The reduction in bacterial adhesion in comparison with the elastomeric substrate was performed through bacterial counts.

2. Experimental section

2.1. Materials

PFM was purchased from Apollo Scientific Ltd. (Stockport, U.K.). D-(+)-Glucosamine hydro-chloride, sodium dodecyl sulfate (SDS), Hellmanex, nitric acid, and silver nitrate were purchased from Sigma-Aldrich. Ethanol was purchased from Scharlab (Barcelona, Spain), a Sylgard 184 kit was purchased from Ellsworth Adhesives (Madrid, Spain) and Si-wafers were purchased from Wafer World (West Palm Beach, FL, USA).

2.2. Methods

Preparation of PDMS samples. PDMS coupons were fabricated as previously described in our group [32]. Briefly, Sylgard 184 kit (10:1) (Ellsworth Adhesives, Spain) was used, using a paint applicator to obtain films of 500 µm thickness on a flat glass plat. Films were incubated at 60 °C overnight and, later, PDMS films were cut in circular pieces of 10 mm diameter to obtain regular coupons. PDMS coupons were washed in 5% SDS solution, rinsed twice with Milli-Q water and, finally, coupons were rinsed and preserved in ethanol 70% until their use. Samples were always removed from ethanol and dried before use by air hose.

2.2.1. Plasma processing

2.2.1.1. Plasma reactor.
Surface modification was performed through a plasma reactor that consisted of a stainless-steel chamber, a vertical plate reactor manufactured by the GEMAT group (Barcelona, Spain) and previously described [17, 32] (Figure S1). Briefly, the ground electrode is the reactor chamber, and the radio frequency electrode is an aluminum plate which is used to hold the samples for polymerization. Gases (argon and oxygen) and monomers (PFM) are supplied via manifold with gas fluxes adjusted with a tree of needle valves. Standard base pressure to all experiments was 6×10^{-4} mbar, and the monomer vapor (PFM) was introduced at a constant pressure of 0.02–0.04 mbar. More information of plasma reactor as well as schematics can be found in supplementary information.

2.2.1.2. Plasma polymerization.
The substrates used in this work were PDMS coupons that were coated with the pp-PFM and to obtain the final silver coated surfaces. Additional silicon wafers were used as controls to validate the reproducibility of the polymerization process. The procedure of plasma polymerizations for these surface modifications was carried out similarly as described in a previous work [17]. Briefly, PDMS coupons and a silicon wafer were placed on the aluminum plate in the center of the reactor. Before introduction of the substrate, the chamber was cleaned in continuous wave O_2/Ar (1:1) plasma for approximately 1 h at a power of 150 W.

Plasma polymerizations were carried out in two steps: First, PFM monomer vapor was flowed into the reactor chamber. After monomer stabilization flow, the continuous radio frequency power was fixed at 15 W, and pulse plasma polymerization (duty cycle of 10/10) was carried out for a desired polymerization time (different polymerization times were studied to obtain different thickness and tortuosity of pp-PFM thin films as shown in Table 1). Plasma discharge was then turned off and PFM vapor flow was kept constant for an additional time (post-polymerization time). After the polymerization process, pp-PFM samples were removed from the chamber and stored until use under argon atmosphere.

Table 1. Plasma polymerization conditions for pp-PFM PDMS modification to obtain specific metallic silver structures.

	Polymerization time/min	Post-polymerization time/min
A–Sharp Blades	3	3
B–Thick Blades	3	10
C–Leaves	10	10

2.2.2. Silver immobilization

After pp-PFM thin film was deposited on the surface of the PDMS, samples were incubated with a glucosamine 1M to immobilize the sugar groups on the polymeric chain to assist the posterior silver reduction. The pH was adjusted to 7.4 for 6 h at least to promote the reaction of pentafluoro phenyl group with glucosamine. After that, samples were washed in Milli-Q water and dried in argon atmosphere. For the silver coating, silver was reduced on surfaces using the Tollens' method (Supplementary materials, Eqs. 1 and S2). Briefly, this method involves the complexation of silver ions with ammonia to obtain diamminesilver (I) ions that can be reduced to metallic silver in a heated bath once in contact with the glucosamine modified surfaces. A concentrated Tollens' reagent was prepared by adding 100 μL of 1 M NaOH to 1 mL of 0.1 *M silver* nitrate, observing the precipitation of the silver oxide. Then, 100 μL of 30% ammonia was added, and the complete dissolution of the precipitate was observed due to the complexation of the silver by ammonia. The modified samples with the attached glucosamine were introduced on a separated vial with 4 mL/vial of the Tollens' reagent and heated on a water bath at 90 °C for the desired time reaction.

2.2.3. Surface characterization

The silver modified surfaces were characterized through water contact angle (WCA; DSA100, Krüss) to evaluate the surface hydrophobicity. Images from surfaces were taken using a Field Emission Scanning Electron Microscopy (FE-SEM, Merlin 0.8 nm to 15 kV with EDS Oxford LINCA X-Max) without Au treatment to enhance the electric conductivity. The surface roughness of the films was measured using the measurements obtained from more than 50 SEM images through ImageJ software (http://www.imagej.nih.gov/) with SurfCharJ plug-in and the local roughness was analyzed using ISO 4287/2000 [33]. Total silver deposited on surfaces and the silver released from surfaces were quantified using an inductive coupled plasma optical emission spectroscopy (ICP, OES Optima 2100 DV, PerkinElmer). Silver samples were treated with nitric acid 30 % and diluted 1:100 in Milli-Q water before using ICP. The protocol from Hohmann et al. [34] was adapted to test the amount of protein adhered to the PDMS surfaces. Fetal-bovine serum (FBS) was used as complex-protein media to test adsorbed proteins to surfaces and after 24 h of incubation, samples were washed with isopropanol twice and Radioimmunoprecipitation assay buffer (RIPA, Sigma-Aldrich®, Germany) buffer was added to samples. Then, samples were incubated during 30 min at 37 °C and Micro BCA™ Protein Assay Kit (Thermo Fisher Scientific®, Spain) was used to quantify the amount of adsorbed protein according using bovine serum albumin (BSA) as a standard.

2.2.4. Assessment of bacteriophobic properties

Strains and bacterial assays. Bacterial strains were purchased from ATCC®, The Global Bioresource Centre in United States of America. The strains used were 1) gram-negative *Pseudomonas aeruginosa* PA01 (ATCC 15692™) as opportunistic pathogen research model that possesses a single unsheathed polar flagellum that plays a variety of roles in the virulence in addition to its central role in swimming motility and adhesion according to ATCC® bank information; 2) *Escherichia coli* CFT073 (ATCC 700928™) gram-negative uropathogenic (clinical isolate), multifimbriae strain with specific fimbrial adhesins according to its genome sequence [35]; and 3) *Staphylococcus aureus* subsp. aureus (ATCC 33592™), gram-positive and multi resistant strain (Gentamicin and Methicillin resistant), all of them with biosecurity level 2. These strains are models to biofilm development, multi resistant pathogens, multi fimbriae bacteria (as attachment and adhesion models) and they are also the commonly found species in hospital HCAIs. A single colony from the stock of each strain was cultured in 50 mL of appropriated growth media (Luria Bertani, (LB) for *E. coli* CFT073 and Tryptic Soy Agar (TSB) for *P. aeruginosa* PA01 and *S. aureus subs. aureus*) at 37 °C with overnight agitation to obtain the initial inoculum.

2.2.4.1. Bacterial viability.
To compare the bacterial growth between the bacteria in contact with PDMS and the bacteria in contact with the coated surfaces, optical density was measured at 600 nm in a spectrophotometer (Spectramax M2, Molecular Devices, USA) between 18 to 50 h at 37 °C. Also, Minimum Bactericide Concentration (MBC) was measured for the three strains used in this work, supplementary information (Figure S2).

2.2.4.2. Bacterial adhesion.
To evaluate bacterial adhesion on surfaces, initial inoculum was diluted in fresh media and grown to OD 0.02 (600 nm). The bacteria were then put in contact with PDMS coupons as control and synthetised/manufactured surfaces as test, in static conditions at 37 °C overnight (20 h). Bacterial extraction protocol was adapted from Mandakhalikar et. al. [36]. After bacterial incubation, samples were removed from wells and washed twice in sterile PBS at room temperature to remove non-attached bacteria. Samples were then placed in sterile tubes with 2 mL of PBS and the tubes were sonicated for 10 min at 70 Hz, vortex for 2 min and sonicated again for 10 min. Empty coupons were discarded. Bacterial pellets were collected at 4,500 g for 20 min, rinsed twice and resuspended in sterile PBS, to perform serial dilutions. Serial dilutions were made in PBS. Bacteria were plated in appropriate agar media to each bacterial strain (LB-agar to plate *E. coli* CFT073 and TSA (TSB-agar) to plate *P. aeruginosa* PA01 and *S. aureus* subs. aureus). Plates were incubated at 37 °C between 18 to 36 h according to each bacterial strain requirements to count total colony forming units (CFUs).

2.2.4.3. Statistical analysis.
Surface-adhesion experiments were performed 3 times and each experiment had 4 replicates (n = 4). Once adhered bacteria had been quantified, a one-way ANOVA test with multiple comparisons was performed. Adhesion to PDMS was used as a control data, obtaining the p-Value parameter as result. These p-Values indicated if the difference between the number of bacteria adhered on PDMS compared with the rest of the samples were significant (P-value > 0.05 (ns, non-significant), P-value < 0.05 (*), P-value < 0.01 (**), P-value < 0.001 (***)). The GraphPad Prims program was used to obtain the results.

2.2.4.4. Bacterial visualization.
To test bacterial adhesion on surfaces by FE-SEM, initial inoculum of *E. coli* CFT073 was diluted in fresh media and grown to OD 0.02 (600 nm) and the bacteria were then put in contact with coupons in static conditions at 37 °C overnight. Surfaces were washed twice in sterile PBS at room temperature to remove non-attached bacteria. The attached bacteria on samples were then fixed adding 4% formaldehyde at room temperature for at least 2 h. Formaldehyde was washed with sterile PBS and a serial dehydration using ethanol 30%, 50%, 70% (30 min each) with a final wash in ethanol 90%. Samples were coated with gold before being observed. Surfaces incubated with bacteria were prepared according to the protocol given by the manufacturer with the kit LIVE/DEAD™ BacLight™ Bacterial Viability kit, L7007 (Thermofisher®, USA) to obtain confocal microscopy images to visualize live or dead bacteria.

3. Results and discussion

### 3.1. Preparation of pp-PFM/silver coating and characterization

The antibacterial effect of metallic silver coating as a release platform immobilized on flexible substrates through plasma-polymerized

pentafluorophenyl methacrylate (pp-PFM) had been previously studied by our research group. Polymeric thin films of pp-PFM consisted of an interesting active coating because of the reactivity of the ester group, which may be used to create a covalent bond with molecules that contain amine groups in their structure [17, 37, 38]. The incubation of pp-PFM thin films with D-(+)-Glucosamine hydrochloride produced the immobilization of the sugar in the pp-PFM backbone, generating a suitable reductive platform capable of obtaining nanostructured metallic silver through Tollens' reaction (supplementary materials). EDX was used to validate that the obtained nanostructures are composed by metallic silver as previously described in literature [17] (Figure S3). In this context, the controlled release of silver ion produced by a local oxidation of silver surface generated an increase of bacterial mortality and partially reduced the bacterial adhesion and colonization [39]. In this work, it was found that, depending on the conditions of plasma polymerization (Table 1), the thickness and the tortuosity of pp-PFM thin film can be controlled and modulated. These changes produced differences in the nanostructure and

the morphology of the immobilized metallic silver layer showing different surface properties. Hence, it was possible to differentiate three nanostructures formed from the silver layer: "Sharp blades", "thick blades" and "leaves" (Figure 1). Among all the conditions that affect the polymerization of PFM, the most critical were the polymerization time (time that PDMS samples were exposed to pp-PFM plasma) and the post-polymerization time (time that pp-PFM vapor were kept constant after the polymerization).

It was found that short times (3 min each) in both, polymerization and post-polymerization process allowed the obtention of thin pp-PFM films, where the nucleation of silver created multiple sharp structures of 200 nm long and a few nanometers wide ("Sharp blades" Figure 1(A.1 and A.2)).

Increasing the post-polymerization time allowed the termination of PFM chain growth after plasma process, which in turn, enabled the reactive points of the plasma polymerized polymer chain to react with the vapor of the PFM and increased the "mountainous region
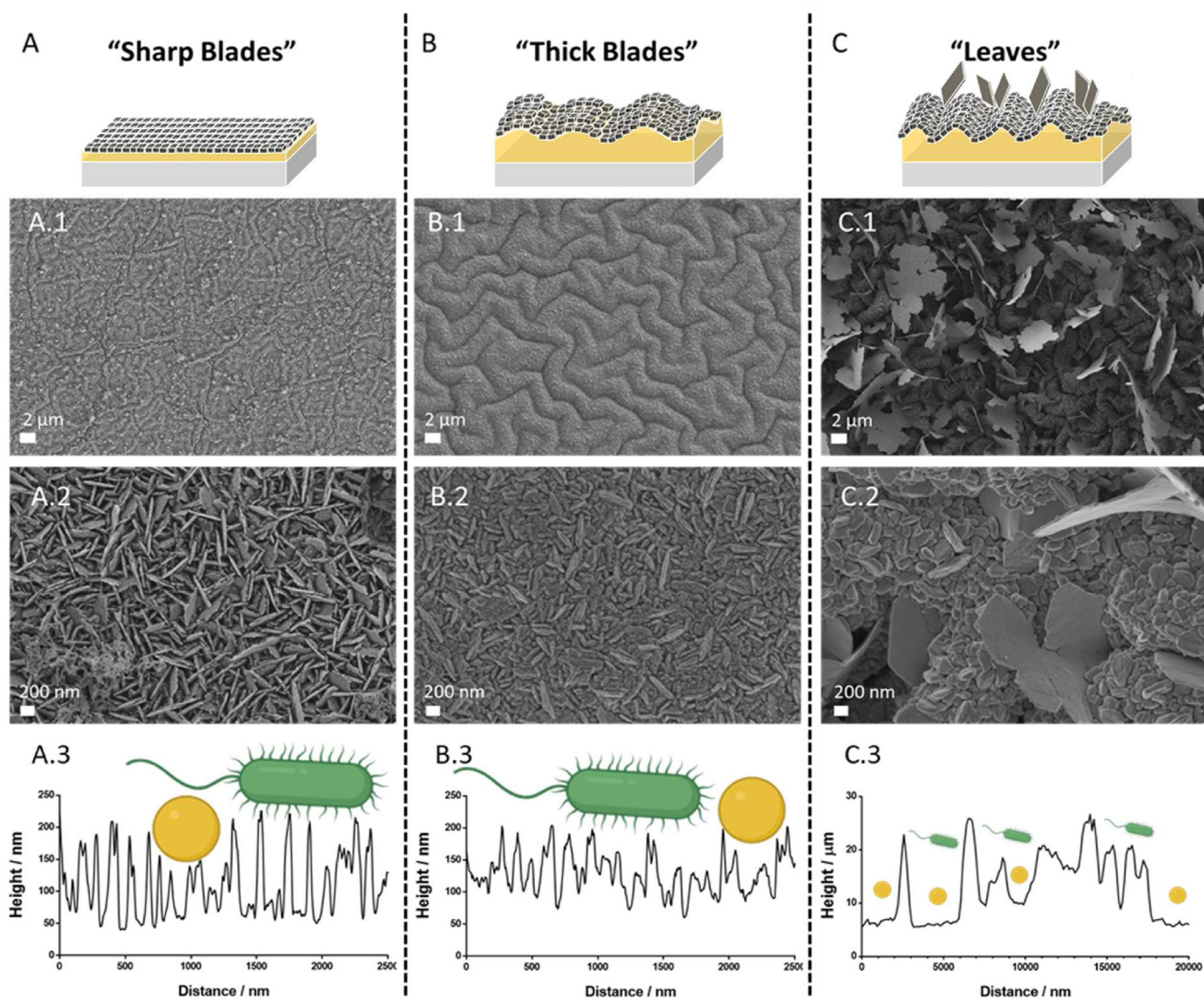
Figure 1. Field emission scanning electron microscopy of three silver surfaces. The graph shows the base silicone (PDMS, dark grey), the pp-PFM coating (yellow) with different shapes according to the tortuosity observed in the FE-SEM images and the silver coating with different morphologies (light grey). Samples were named according to the pp-PFM tortuosity and the nanostructure observed on their surface. A surface with "sharp blades" (A, A.1 and A.2), a surface with "thick blades" (B, B.1and B.2) and a surface with "leaves" (C, C.1, and C.2). The mechanism underlying the influence of surface morphology on bacteria adhesion was based on the roughness profile of "sharp blades" (A.3), "thick blades" (B.3) and "leaves" (C.3) morphology. Scheme of the bacteria is shown to scale in relation to the roughness profile.

morphology", in which peaks and valleys were clearly more recognizable, about 2–4 μm (Figure 1-B.1). After silver nucleation, the result was similar to that shown in the previous surface but, in this case, the "blades" were obviously wider in comparation with the previous structure and were thus named "thick blades" (Figure 1-B.2). Higher polymerization and post-polymerization times (10 min) resulted in a more complex structure due to an increase in pp-PFM chain tortuosity. In this case, silver nucleation sites led to the generation of silver leaves covering the main surface (Figure 1-C.1) with a thickness of less than 50 nm. Behind the "leaves" structures, it can be observed that the "mountainous region morphology" was maintained but, unlike the leaves morphology, a significant particle growth was observed with nanoparticles higher than 200 nm (Figure 1-C.2).

The roughness profile of studied surfaces was performed to evaluate the ability of the morphology to create unfavorable conditions for bacterial adhesion and to elucidate a hypothesis for the antibacterial—bacteriophobic mechanism. Figure 1-A.3 shows the roughness profile for a representative region of the sharp blades surface. The profile confirms the presence of blades with a height of 150 nm and a distance between blades less than 100 nm, while thick blades present a similar roughness profile (Figure 1-B.3) with blades about 100 nm in height separated by less than 80 nm. Previous reports indicated that physical impediments led by the roughness of the surface topography may play an interesting role in avoiding bacteria interaction and attachment [40]. Figure 1–A.3 and B.3, shows a schematic of the bacteria-surface interaction indicating how multiscale wrinkled surfaces can impede bacterial attachment due to the limited surface area available.

The characterization of the "leaves" structure is much more complex due to its amorphous morphology led by silver nucleation, showing a micro- and nano-roughness formed by slender "leaves" of 10 μm in height and a thickness of less than 50 nm with a separation between the leaves that can be higher than 2 μm (Figure 1-C.3). Initially, in this case, bacterium can easily interact with the surface due to the separation between the leaves. However, once the bacteria reach the surface, the effect of the nanostructure must be evaluated.

Surface hydrophobicity was studied because it can play and important role in the bacterial adhesion mechanism. It is known that rough surfaces with low hydrophobicity present more sites for bacterial attachment [21, 41] providing protection from the shear forces produced by the exposition to biological medium [42]. With this phenomenon in mind, water contact angle (WCA) of the silver surfaces was measured using uncoated PDMS coupon as control (Figure 2A). PDMS samples showed a characteristic WCA around 95° indicating a well described hydrophobic behavior of silicone. However, the modified surfaces revealed a WCA around 150° indicating that these surfaces were in the range of super-hydrophobicity.

The nano-structuration of the silver surfaces present a high accentuated roughness that contributes to increasing the hydrophobicity to super-hydrophobic range. As described in the literature, the combination of nanostructured rough surface with super-hydrophobic behavior may act as an antifouling surface and/or promote the air entrapped beneath the liquid in the topography and therefore reduce the bacterial adhesion obtaining a bacteriophobic effect [41, 43, 44, 45].

Once hydrophobicity was studied, the amount of total silver deposited on surfaces was evaluated. It is interesting to highlight that the developed surfaces presented the same amount of silver as shown in Figure 2B, regardless of the complexity of their structure. These results indicate that super-hydrophobicity behavior is not achieved due to an increase of the amount of silver in the surface but by a redistribution of how this silver has been anchored to it. Consequently, all changes produced by the surfaces on bacterial adhesion are associated with a nano-structuration of the silver surface.

Modified surfaces were incubated in Fetal Bovine Serum (FBS) to quantify protein adsorbed on the surface. As can be seen in Figure 2C, the pp-PFM-silver modified surfaces significantly reduced the total amount of adsorbed protein in comparison with uncoated silicone. Considering that the presence of proteins on the surface promotes stable interactions with bacteria, the studied surfaces not only present a physical impediment to avoid adhesion but also reduce the interaction protein-bacteria on the surfaces, limiting bacterial adhesion [46, 47]. Because of these results, it is expected that this low-protein interaction combined with the physical impediments of the micro/nano—structure promote a long-lasting bacteriophobic effect.

As we previously described in bibliography [48], polymer CVD techniques are compatible with any substrate not affected by reduced pressure and can coat fragile substrates such as sensors [49] and complex geometries such as particles [49, 50] or trenches [48], as well as elastic and elastomeric substrates [17], so the recreation of these nanostructures on the surface of a medical device with minimal process adjustments must be very easy.

3.2. Silver ions release and its effect on bacterial growth

The release of silver ions from the silver surfaces plays an important role in the bacterial adhesion mechanism and in the bacteriostatic/bactericide effect of the surface [51, 52]. The amount of silver released to medium can provide an idea of the contribution of silver ions to bacteria elimination, i.e., lower concentrations of silver ions may imply a major contribution of the surface nano-structuration on bacterial adhesion reduction. After the Tollens' reaction, the formed surfaces were composed by a continuous metallic silver layer in contrast to the antibacterial surfaces formed through the union of silver nanoparticles, where the release of a high amount of colloidal silver is promoted. To evaluate the accumulated silver ions released in media from the three developed silver surfaces, 1 mL of each sample was taken from media (and replaced with fresh media) at different time points during 530 h and analyzed by ICP (Figure 3A). To exclude that silver ion release was caused by chemo-adsorbed silver during the Tollens reaction, silver release profiles were also obtained immersing the samples in acetic acid (Figure S4).
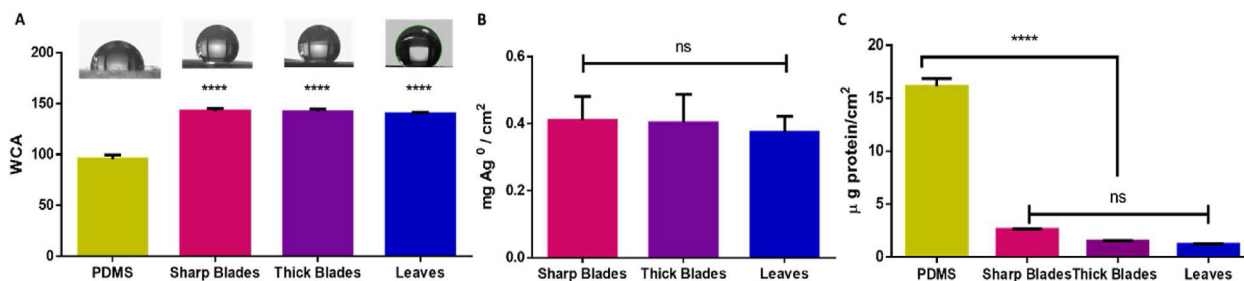
Figure 2. Water contact angle of the developed silver surfaces compared with uncoated PDMS (A) and silver quantification by cm^2 for each silver surface tested by ICP (B). Amount of protein adsorbed on the surfaces by cm^2 after 24 h of incubation with Fetal Bovine Serum (C). Statistical analysis indicated a significant difference between control and all three surfaces, with a minimum p-value of <0.05 (*) and a maximum p-value of <0.001 (***).
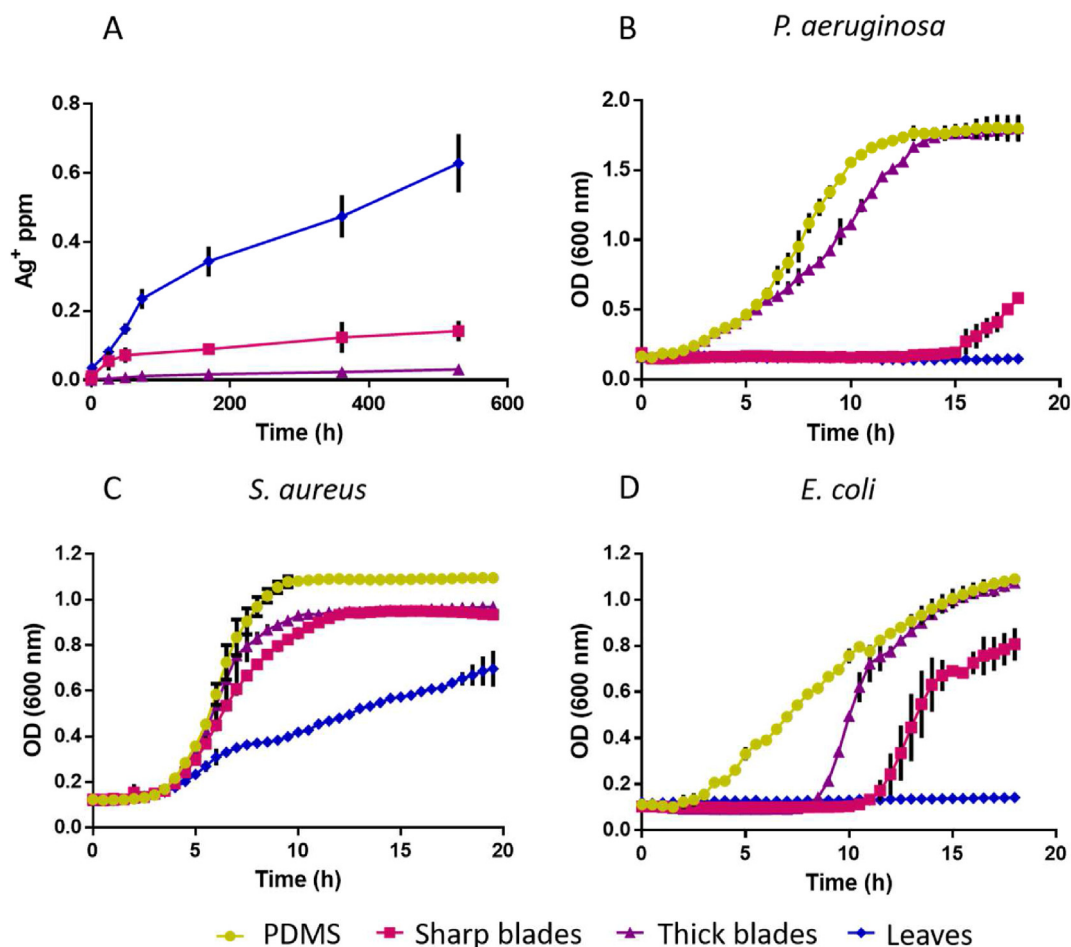
Figure 3. Accumulative release of silver ion from silver surfaces (A) and growth curves of *P. aeruginosa* PAO1 (B), *S. aureus* subs. aureus (C) and *E. coli* CFT073 (D) in contact with PDMS as control surface and the three surfaces with "sharp blades", "thick blades" and "leaves".

It is interesting to note that the three silver surfaces with different nano-structuration presented different profiles of silver ions release. On the one hand, the surface with "leaves" morphology revealed an initial burst release of 0.23 ± 0.03 ppm during the first 72 h followed by a change in the slope of the release profile (Figure 3A). This behavior may be explained by local oxidation reactions of silver leaves with the oxygen in the bacteria media, which is promoted by the high specific surface of the leaves morphology. In this sense, the first stage of the release corresponds with the silver release of poorly attached thin leaves (first 72 h), followed by a sustained release of thicker leaves (from 72 h to endpoint). After 530 h of study (22 days), the release of silver ions did not reach a plateau indicating that silver leaves were a significant silver reservoir. On the other hand, "sharp blades" (Figure 3A), showed an initial minimum burst release of 0.05 ± 0.02 ppm during the first 24 h of incubation, followed by a sustained release that almost reached the plateau. These differences can be explained because the "sharp blades" structure was less exposed to media than silver "leaves", and therefore less exposed to local oxidation, presenting a sustained release of silver ions. Finally, the "thick blades" morphology showed a silver ion release below previous surfaces and being close to the quantification limit of the analytical method (10 ppb). This effect may be attributed to the blade thickness as well as to the tortuosity of the silver layer that protects the stability of silver blades making them more resistant to oxidation. Considering these results, it can be concluded that the "thick blades" structure does not produce the release of silver ions in a significant way.

In order to evaluate the effect of the different silver ion release profiles, the different silver surface samples were put in contact with three different bacterial strains to study their growth evolution: *Pseudomonas*

aeruginosa PA01, *Staphyloccocus aureus* subs. aureus and *Escherichia coli* CFT073 (Figure 3B, C and D).

As can be observed, bacterial growth profile showed several differences regarding the exposed released silver ions. The ions released from surface with the "leaves" morphology revealed a standard bacteriostatic behavior on gram-negative strains (*P. aeruginosa* and *E. coli*) completely avoiding the bacterial growth (Figure 3B and C). However, a delay in bacterial growth was observed on gram-positive strains such as *S. aureus*. These behaviors are consistent with the silver release profile observed for the "leaves" morphology, where a high amount of silver ions was released into the medium, affecting bacterial duplication and viability. To demonstrate that the bacteriostatic effect observed with "leaves" surfaces was maintained over time, all the growth curves (*P. aeruginosa* and *E. coli,* and gram-positive *S. aureus)* were extended up to 50 h. No bacterial growth was observed in the case of gram-negative strains, and gram-positive did not reach the stationary phase (absorbance values of end point measurements shown in supplementary materials, Figure S5). To provide some insight into bacteriostatic or bactericidal effect of the "leaves" surface after 18 h of incubation, an isolated sample of the test medium was collected and cultivated overnight in fresh medium. Absorbance data through time was measured to evaluate if the bacteria had been eliminated (antibacterial behavior) or remained alive but with attenuated replication (bacteriostatic effect). On one hand, erratic bacterial growth profile was observed in the *E. coli* and P. aeruginosa species indicating an inhibitor effect of the surface on gram-positive strains. On the other hand, absorbance values of *S. aureus* were significantly low indicating that bacteria population was dramatically reduced but not completely eliminated. This behavior suggested that silver ion diffusion

does not allow the total elimination of the bacteria present in the media and the surface cannot be considered bactericidal. This effect is completely consistent with the literature regarding silver ion affection on gram-positive strains [22, 51] because gram-positive species present a bacterial wall composed of several layers of peptidoglycan with a thickness 15–80 nm that makes it difficult for silver ions to interact with the respiratory chain, secretion systems or other components of inner membrane [53]. In this sense, the presence of this wall reduces the efficacy of antimicrobial effect of silver ions.

In contrast, the released silver ions from surface with "sharp blades" morphology presented a different behavior compared with the "leaves" morphology due to the general reduction of silver ion release profile. Thus, a delay was observed at the beginning of the exponential phase in bacterial growth (Figure 3B, C and D) that can be associated with the initial burst release of silver ion (Figure 3A). This silver burst avoided the bacterial duplication, but it did not affect growth completely. Once the bacteria had replicated enough to overcome the silver ion effects, bacteria were able to overcome the effect of the released silver and began their exponential growth phase. It was observed that this effect was more attenuated in *S. aureus* (Figure 3C). If the incubation times are extended to 50 h in *P. aeruginosa* and *E. coli*, the growth curves reach the stationary phase, almost matching the PDMS control (Figure S5), which indicates that while silver ion release is not able to kill bacteria, it slows bacterial growth.

The released silver ions from "thick blades" morphology did not present any effect on bacterial growth in any bacterial strain (Figure 3). However, a lengthening on the adaptation phase in *E. coli* was observed reaching a stationary phase at the same time as the control at 18 h period, a profile considered as normal growth. These results are consistent with the silver ion release profile revealed in Figure 3A, where the "thick blades" surface did not release significant amount of silver ions to the medium. This result is especially interesting because any variations in bacterial adhesion on this surface will not be able to be associated with the effect of silver ion on bacteria but only on the interaction between bacteria and the surface morphology.

Finally, in addition to recovering bacteria from the medium and growing them, in order to verify that bacteria were inhibited but not dead, MBC tests were performed. MBC tests were made to determine the minimum bactericidal concentration using silver (Figure S2). Noting that the accumulative release of silver at 22 days (Figure 3A) would not be enough to kill the bacteria completely in any case.

From a cytotoxic point of view, the daily release of silver from "sharp blades", "thick blades" and "leaves" surfaces do not represent a concern. The amount of released silver in the medium did not exceed 0.1 ppm/day (Figure 3A). This maximum concentration is agreed for human consumption of silver dissolved in water by the World Health Organization (WHO/HEP/ECH/WSH/2021.7 report). There is little information on the health effects of skin exposure to silver compounds. There have been no cases of argyria derived from the use of lotions or medical devices with high concentrations of silver. Concentrations of up to 81 ppm silver/day in contact with the skin is allowed according to the Agency for Toxic Substances and Disease Registry (Silver CAS#7440-22-4 report). So, all the proposed surfaces, including "leaves" surface, could be implemented in implantable devices or in close contact with the skin.

3.3. Bacteriophobic effect characterization

In order to characterize how the nano-structured silver surfaces affect the bacterial adhesion after incubation with the developed samples, FE-SEM microscopy, live and dead staining, and bacterial counts with the same bacterial strains studied in Figure 3 were performed.

First, samples were observed by FE-SEM after bacterial incubation (Figure 3) *E. coli* (Gram negative) and *S. aureus* (Gram positive) were selected to show its attachment on metallic silver surfaces because they are reference strains in the field of clinical pathogens due to their specific appendages that interact with tissues and surfaces [54, 55]. Non

modified PDMS was used as a control (Figure 4A) revealing a uniform, homogeneous and stratified layer of bacteria, indicating that bacteria had been adhered on the surface without difficulty. *E. coli* were disposed randomly on PDMS indicating that bulk PDMS surface topography did not produce a specific orientation effect on bacterial adhesion. Also, bacterial division could be observed indicating that bacteria were metabolically active on PDMS substrates. Signs of bacterial preference to be anchored on specific areas of the PDMS such as, a specific orientation of bacteria, bacteria-free areas or deformations in bacteria structure were not observed.

In contrast to PDMS behavior, the surface with "sharp blades" morphology (Figure 4B) incubated with *E. coli* revealed significantly less attached bacteria than PDMS control. Bacteria were randomly attached without showing a specific orientation. It was also observed that "Sharp blades" surface promotes the bacteria elimination through closely physical interaction with the surface topography. This behavior was previously observed in literature in physical antimicrobial surfaces describing how morphology can disrupt bacterial membranes [27, 56]. A more detailed picture of the bacterial morphology on this surface can be seen in supplementary information (Figure S6). Considering that the formation of bacterial aggregates or microcolonies were not observed on all "sharp blades" samples, the anchored bacteria may be attributed to random bacterial attachment. This effect can be explained as a combination of the physical impediment caused by the roughness of the surface (Figure 1-A.3), the topography of the blades that can allow a disruption of the bacterial membrane as previously reported [27] and super-hydrophobic behavior (Figure 2A). In this way, surfaces with "thick blades" morphology (Figure 4C) presented bacterial orientation according to the valleys of the grooves, preferring to anchor themselves to these grooves instead of to the tops. These bacteria did not present structural membrane damage or affected volumes indicating no membrane disruption. Instead, bacteria seemed to be not able to find a suitable anchoring site because there were significantly less adhered bacteria than on the PDMS control and with similar morphology to "sharp blades". Considering that this surface did not present a release of silver ions, this effect can be attributed mostly to a combination of the morphology and super-hydrophobic behavior of the metallic silver nano-blades (bacteriophobic effect), Figure 1-B.3 and Figure 2A. Therefore, because of the nanostructure of the coating, bacteria were not able to properly attach to the surface, being anchored by weak interactions. In this way, bacteria can be detached from the surface returning to the medium and avoiding the adhesion process and the formation of biofilm. Similarly, *S. aureus* was poorly attached to surfaces as well as *E. coli* compared with adhere bacteria to PDMS controls. Small amounts of precipitates, cell debris or spherical aggregates were observed on the "thick blades" and "sharp blades" surfaces (Figure 4F, and G). However, it is interesting to note that the presence of *S. aureus* observed through FE-SEM was practically zero, indicating that "thick blades" and "sharp blades" may represent a good solution to avoid the adhesion of Gram positive bacteria such as *S. aureus*. Finally, Figure 4D, shows the image of the "leaves" morphology surface after being incubated. As can be observed, the "leaves" structures were unhooked after the incubation with bacteria. Remains of these "leaves" structure can be seen on the surface, showing holes and eroded areas caused by medium exposition. The erosion also revealed the characteristic "mountainous" structure, where the grooves presented more tortuosity than previously observed in the other metallic structures. In this way, the "leaves" structures may have been formed through a nucleation process being an extension of the nano-blades present on the others surfaces. These leaves were weakly anchored to the main silver layer resulting in a dynamic surface where, after exposition to a medium, the silver "leaves" were detached producing an actively release of silver (in ionic form). This massive release of silver affected the bacterial growth showing aberrant bacterial growth dynamics or inhibiting all strains as previously observed in the growth curves (Figure 3). The same effect is observed when "Leaves structure" was incubated with *S. aureus* (Figure 4H). The images revealed a small amount of adhered bacteria randomly distributed on the surfaces
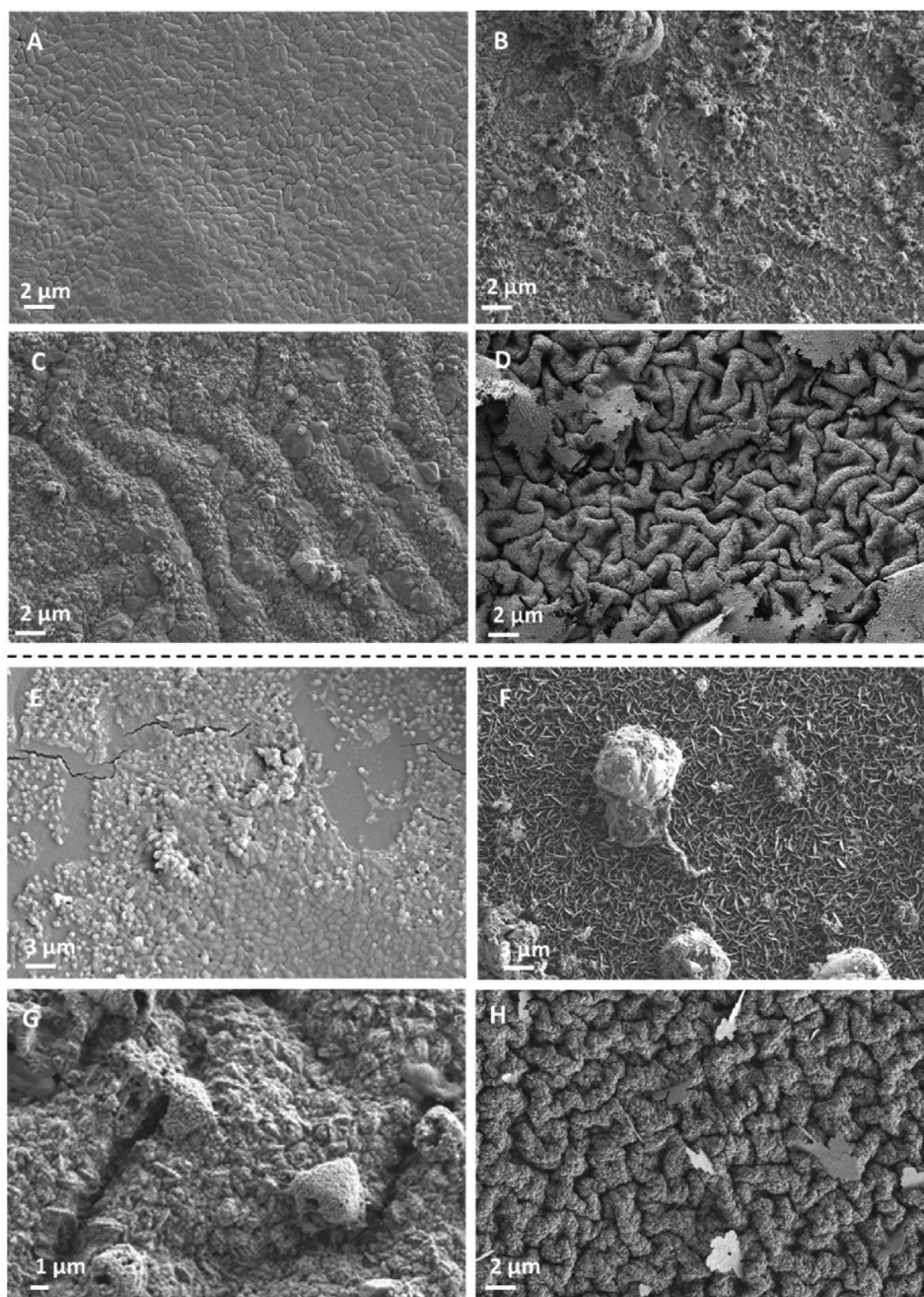
Figure 4. Field emission scanning electron microscopy images. PDMS as a control surface (A,E), surface with "sharp blades" (B,F), surface with "thick blades" (C,G) and surface with "leaves" (D,H) were incubated with *E. coli* CFT073 (upper images) and *S. aureus* (lower images). *E. coli* were artificially painted in green to improve their visualization.

and the structures that predominated were the spherical precipitates. Due to the structural changes produced on the surface after being exposed to bacteria media, FE-SEM images do not provide conclusive information about how bacteria interact with the "leaves" morphology. However, the surrounding bacterial behavior to silver "leaves" detachment could be observed through confocal microscopy with the possibility to discern between living and dead bacteria (Figure 5).

To evaluate the behavior of bacteria surrounding the "leaves" morphology surface, PDMS was used as a control with *P. aeruginosa* as a gold standard strain to study the bacterial attachment (Figure 5A). The surface with "leaves" morphology was incubated with, *E. coli* (Figure 5B), *S. aureus* (Figure 5C) and *P. aeruginosa* (Figure 5D) to show total bacterial deposition discriminating between live attached bacteria, microcolonies and dead attached or deposited bacteria. PDMS in Figure 5A showed a

layered and stratified biofilm, composed mostly of live bacteria (in green). Bacteria were attached to the surface extensively and, after adhesion, bacteria began to divide and secrete extracellular matrix, forming a microcolony, a platform where bacteria are promoted. With enough incubation time, these microcolonies will form a structured biofilm.

The silver "leaves" structure presented a very different behavior compared with the PDMS control. *E. coli* and *P. aeruginosa* had similar bacterial growth in the presence of silver ions, as previously mentioned in Figure 3, but showed a different ability to be adhered to the silver "leaves" surface. Figure 5B revealed a clear surface without observing adhered bacteria. Despite *E. coli* presenting a high amount of pili and specific adhesion mechanisms, once exposed to the silver "leaves" structure, bacteria were unable to overcome the barrier of local release of silver ions and the potential effect of the surface morphology, nano-
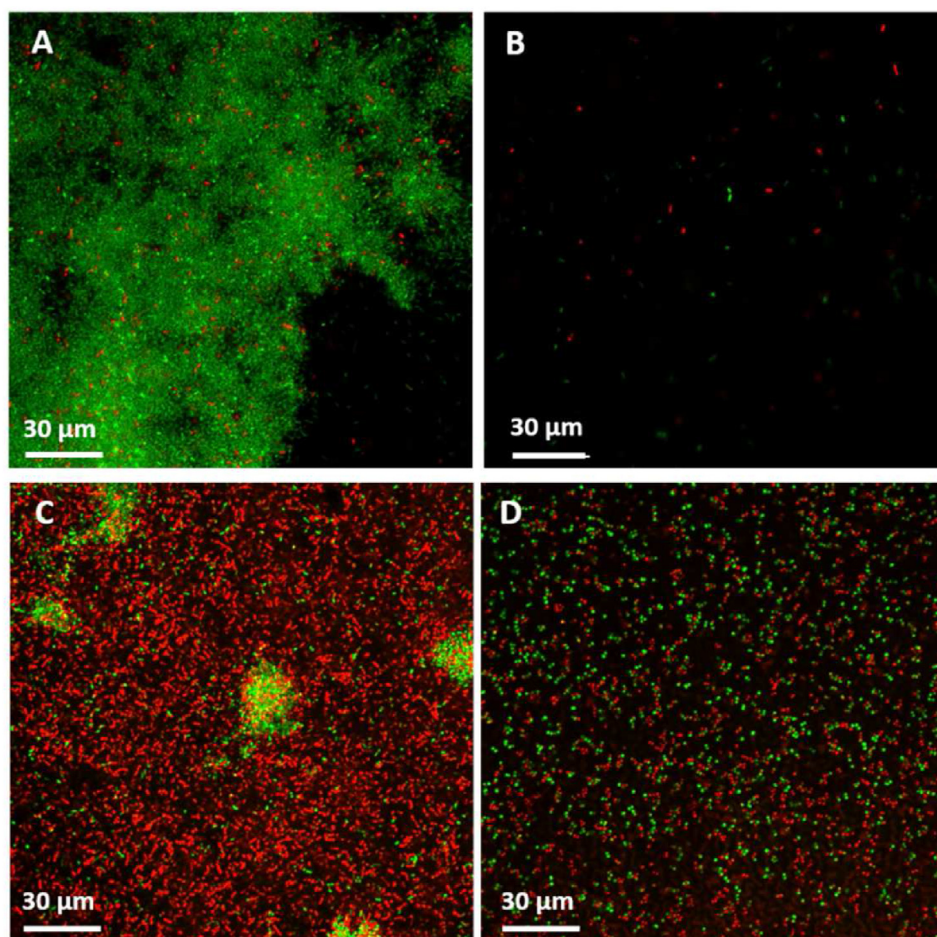
Figure 5. Confocal microscopy of PDMS incubated with *P. aeruginosa* (A) and surface with silver "leaves" incubated with and *E. coli* (B), *S. aureus* (C) and *P. aeruginosa* (D). Samples were stained with a Live & Dead cell staining kit: red dye shows dead bacteria with membrane damage and green dye shows live and metabolically active bacteria, biofilm matrix was not stained.
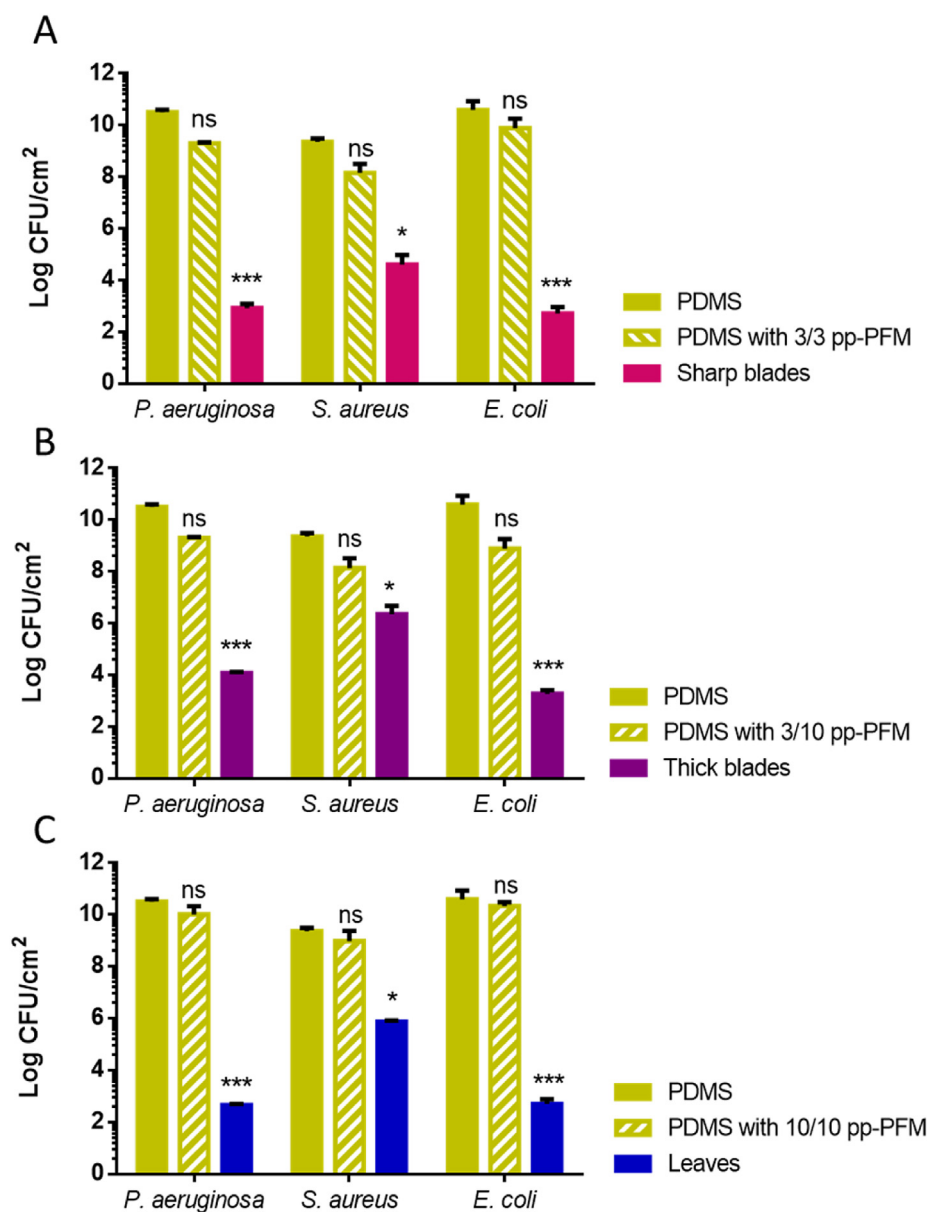
roughness (Figure 1-C.3) and super-hydrophobic behavior (Figure 2), where remaining leaves may produce a bacteriophobic effect in a similar way as observed in the other silver surfaces. By contrast, *P. aeruginosa* (Figure 5C) was able to adhere to the surface, as can be seen in the high concentration of bacteria in the image, but attached bacteria was found dead (red bacteria), probably because of the effect of the released silver ions. As shown in Figure 4, bacteria were attached individually and showed no signs of biofilm formation. However, early stage microcolonies (green clusters) were observed among the dead bacteria. It seems that the erosion of the surface reduces the surface ability to avoid bacterial attachment. Finally, *S. aureus* sub. aureus, shown in Figure 5D, presented a homogeneous attachment of bacteria on the silver metallic surface, where the attached bacteria were partially live and dead almost in equal parts. This high number of attached bacteria was expected considering that *S. aureus* growth is less affected by the release of silver ions and therefore, more suitable to be adhered on the surface. Despite bacteria being localized on top of silver surfaces through confocal microscopy, it is important to highlight that bacterial adhesion was punctual and reversible. Individual bacterium with no connection between them was observed and no indication of bacterial cluster formation was shown and therefore, the development of a biofilm on the surface was improbable.

The next step in the evaluation of the developed surfaces was the quantification of the total amount of living bacteria onto the surfaces to validate the ability of the coating to avoid surface colonization. Samples were placed in medium with different bacterial strains. Bacteria were incubated to ensure bacterial growth and the interaction with the surfaces for 20 h. Samples were then washed to remove weakly adhered bacteria and the remaining bacteria were extracted, plated, and counted considering that each bacterium, alive and able to replicate, can generate a colony forming unit (CFU). Results are shown in Figure 6 for each strain used: *E. coli*, *P. aeruginosa* and *S. aureus*, growth in each proposed surface: "sharp blades", "thick blades" and "leaves", using PDMS and PDMS coated with pp-PFM for each proposed surface as the adhesion reference control.

As can be seen in Figure 6, the three developed surfaces showed a significant reduction of the adhered bacteria for each bacterial strain, revealing a reduction of 3 logarithms at least in the worst case (*S. aureus* on surface with "thick blades") and 8 logarithms in the best case (*P. aeruginosa* on surface with "leaves") in contrast with the uncoated PDMS and PDMS/pp-PFM controls. Despite silver surfaces presenting different mechanism to avoid bacterial adhesion as well as the intrinsic differences of bacterial strains, the bacterial adhesion reduction was similar for each case.

For the *P. aeruginosa* and *E. coli* strains, the presented surfaces represent a highly efficient method to avoid bacterial adhesion, reducing adhesion by more than 6 orders of magnitude. We hypothesize that this effect is mainly produced by a disruption of the bacterial outer membrane, achieved by the action of the surface morphology combined with the release of silver ions, which makes bacteria feel uncomfortable next to the surface. It is interesting to note that the surface with the "thick blades" morphology (Figure 6B), which does not present an ion release profile, reached a similar adhesion reduction value similar to the other surfaces, indicating that the bacteriophobic effect developed only with a surface based approach, can be as efficient as the release of silver ions, the bactericide surface.

A

B

C

Gram-positive bacteria (*S. aureus)* revealed higher adhesion on the silver surface. This behavior can be explained due to the nature of *S. aureus* cell wall and membrane systems. *S. aureus* has a rigid peptidoglycan outer membrane that is harder to disrupt than the gram-negative bacteria outer membranes [31]. In this way, the silver ion released from the "sharp blades" and "leaves" structures (Figure 6A and C) did not affect the growth of *S. aureus,* increasing the bacterial population in the media offering more opportunities for bacteria to interact with the surface and to be adhered. However, the "sharp blades" (Figure 6A) surface showed better *S. aureus* adhesion reduction, which may indicate that the silver ions in combination with a nanostructured surface are capable of disrupting the surface membrane and represent an optimal approach to avoid bacterial adhesion.

Interestingly, bacterial adhesion counts indicate a greater presence of bacteria than those observed by FE-SEM microscopy. Our interpretation is that the adhesion test counts reflect slightly higher orders of magnitude due to the presence of bacteria that were not fully anchored to the surface. This fact highlights the need to always include a microscopy analysis to study bacterial colonization on surfaces.

Despite the fact that the three developed surfaces ("sharp blades", "thick blades" and "leaves") showed an outstanding bacteriophobic behavior, regardless of their effect on bacterial growth, all three surfaces had different bacterial repulsion mechanisms based on their nanostructure, with different effects depending on the bacterial strains. As a result, further studies are required to study these mechanisms in greater depth. It is also interesting to note that in medical devices the bacteria responsible for biofilm formation contacts the surface of the medical device during the implantation [26, 57]. So, in this scenario, the three studied silver nanostructures avoid significantly the bacteria adhered at least during the during the first 20 h after the surface contacts the bacteria inoculum being a promising strategy to avoid the colonization and formation of biofilm.

4. Conclusion

In this work we have studied metallic silver coating immobilized on a pp-PFM thin film. We observed that by modifying the properties of the pp-PFM thin film, structural changes were produced on the metallic silver coating affecting its morphology and therefore how bacteria interact and adhere to the surface. In this regard, by modifying the polymerization conditions of pp-PFM, we identified three different silver morphologies

with three different associated behaviors against bacteria: a "Leaves structure", with a high specific surface morphology that allowed the release of a high amount of silver ions capable of producing a low bactericide effect; a "thick blades structure", a meandering surface with nanometric blades that prevented bacterial adhesion due to a topography-based effect (also called bacteriophobic effect); and a "sharp blades structure" with sharpest nanometric blades that in combination with the topography effect and the disruption of the bacterial membrane presented both bacteriophobic and bacteriostatic effects. The three developed strategies against bacteria revealed an outstanding potential to avoid bacterial adhesion, revealing more than 6 orders of magnitude in CFU reduction on bacterial counts compared with the same surface without the metallic surface. This effect, along with the fact that these silver surfaces can be easily used to coat all kinds of materials, including elastomeric ones that are more challenging to coat, indicate that these strategies show great potential as a solution to avoid bacterial colonization as well as biofilm formation on medical devices.

5. Supporting information

Schematic diagram of stainless-steel vertical plasma reactor and its electrical components. The surface modifications carried out in this work were performed using a stainless-steel vertical plasma reactor manufactured by the GEMAT group (IQS-URL, Barcelona).

- Manufacture of silver-based nanostructured surfaces, chemical reactions equation.
- Energy Dispersive X-Ray Analysis (EDX) of surfaces after manufacturing.
- Accumulative silver release in acetic acid. To demonstrate that silver released from the surfaces is mostly due to the local oxidation of the surface, chemo-adsorbed silver was studied by a release test performed in acetic acid.
- Bacterial growth curves, end point measurements. Growth curves were extended up to 50 h to demonstrate the effect of all proposed surfaces on bacterial growth at long times.
- Minimum bactericide concentration (MBC) of silver for the tested strains.
- FE-SEM image of bacterial membrane damage
- SEM image of pp-PFM surfae before silver deposition

Declarations

Author contribution statement

Cristina García-Bonillo, Robert Texidó: Conceived and designed the experiments; Performed the experiments; Analyzed and interpreted the data; Wrote the paper.

Joan Gilabert-Porres, Salvador Borrós: Conceived and designed the experiments; Analyzed and interpreted the data; Contributed reagents, materials, analysis tools or data.

Funding statement

Data availability statement

Data will be made available on request.

Declaration of interests statement

Tractivus is a company that work in the development of antifouling surfaces. However, Tractivus does not have any commercial interest in the results presented in this paper. The patent is related with the development of antifouling surfaces, but the paper submitted is basic science and it is not useful for strengthening the patent. Thus, the authors confirm that there are no known conflicts of interest associated with this publication and there has been no significant financial support for this work that could have influenced its outcome.

Additional information

Supplementary content related to this article has been published online at https://doi.org/10.1016/j.heliyon.2022.e10842.

Acknowledgements

References

[1] H.A. Khan, A. Ahmad, R. Mehboob, Nosocomial infections and their control strategies, Asian Pac. J. Trop. Biomed. 5 (7) (2015) 509–514.
[2] R.M. Klevens, J.R. Edwards, C.L. Richards, T.C. Horan, R.P. Gaynes, D.A. Pollock, D.M. Cardo, Estimating health care-associated infections and deaths in U.S. Hospitals, 2002, Publ. Health Rep. 122 (2) (2007) 160–166.
[3] World Health Organization, The burden of health care-associated infection worldwide: a summary, World Heal. Organ. 3 (2011).
[4] M. Haque, M. Sartelli, J. McKimm, M.A. Bakar, Health care-associated infections – an overview, Infect. Drug Resist. 11 (2018) 2321–2333.
[5] A.S. Letica-Kriegel, H. Salmasian, D.K. Vawdrey, B.E. Youngerman, R.A. Green, E.Y. Furuya, D.P. Calfee, R. Perotte, Identifying the risk factors for catheter-associated urinary tract infections: a large cross-sectional study of six hospitals, BMJ Open 9 (2) (2019) 1–7.
[6] M. Zaborowska, K. Welch, R. Branemark, P. Khalilpour, H. Engqvist, P. Thomsen, M. Trobos, Bacteria-material surface interactions: methodological development for the assessment of implant surface induced antibacterial effects, J. Biomed. Mater. Res. Part B Appl. Biomater. 103 (1) (2015) 179–187.
[7] H. Straub, C.M. Bigger, J. Valentin, D. Abt, X.H. Qin, L. Eberl, K. Maniura-Weber, Q. Ren, Bacterial adhesion on soft materials: passive physicochemical interactions or active bacterial mechanosensing? Adv. Healthc. Mater. 8 (8) (2019) 1–8.
[8] J. Gutman, S.L. Walker, V. Freger, M. Herzberg, Bacterial attachment and viscoelasticity: physicochemical and motility effects analyzed using quartz crystal microbalance with dissipation (QCM-D), Environ. Sci. Technol. 47 (1) (2013) 398–404.
[9] G. Feng, Y. Cheng, S.Y. Wang, D.A. Borca-Tasciuc, R.W. Worobo, C.I. Moraru, Bacterial attachment and biofilm formation on surfaces are reduced by small-diameter nanoscale pores: how small is small enough? NPJ Biofilms Microbiomes 1 (May) (2015).
[10] C. Garcia-Bonillo, R. Texido, G. Reyes-Carmenaty, J. Gilabert-Porres, S. Borrós, C. García-Bonillo, R. Texidó, G. Reyes-Carmenaty, J. Gilabert-Porres, S. Borrós, Study of the human albumin role in the formation of bacterial biofilm on urinary devices using QCM-D, ACS Appl. Bio Mater. 3 (5) (2020), 0c00286.
[11] H.-C. Flemming, J. Wingender, U. Szewzyk, P. Steinberg, S.A. Rice, S. Biofilms Kjelleberg, An emergent form of bacterial life, Nat. Rev. Microbiol. 14 (9) (2016) 563–575.
[12] I.U.K. Altaf, A. Khan, A. Mahboob, Antimicrobial resistance and a diminishing pool of reserved antibiotics, Sao Paulo Med. J. 137 (4) (2019) 384–385.
[13] E. Tacconelli, E. Carrara, A. Savoldi, S. Harbarth, M. Mendelson, D.L. Monnet, C. Pulcini, G. Kahlmeter, J. Kluytmans, Y. Carmeli, et al., Discovery, research, and development of new antibiotics: the WHO priority list of antibiotic-resistant bacteria and tuberculosis, Lancet Infect. Dis. 18 (3) (2018) 318–327.
[14] J.N. Pendleton, S.P. Gorman, B.F. Gilmore, Clinical relevance of the ESKAPE pathogens, Expert Rev. Anti Infect. Ther. 11 (3) (2013) 297–308.
[15] A. Penesyan, I.T. Paulsen, M.R. Gillings, S. Kjelleberg, M.J. Manefield, Secondary effects of antibiotics on microbial biofilms, Front. Microbiol. 11 (2020) 1–8.
[16] C. Adlhart, J. Verran, N.F. Azevedo, H. Olmez, M.M. Keinänen-Toivola, I. Gouveia, L.F. Melo, F. Crijns, Surface modifications for antimicrobial effects in the healthcare setting: a critical overview, J. Hosp. Infect. 99 (3) (2018) 239–249.
[17] J. Gilabert-Porres, S. Martí, L. Calatayud, V. Ramos, A. Rosell, S. Borrós, Design of a nanostructured active surface against gram-positive and gram-negative bacteria through plasma activation and in situ silver reduction, ACS Appl. Mater. Interfaces 8 (1) (2016) 64–73.
[18] J.P. Ruparelia, A.K. Chatterjee, S.P. Duttagupta, S. Mukherji, Strain specificity in antimicrobial activity of silver and copper nanoparticles, Acta Biomater. 4 (3) (2008) 707–716.
[19] K. Punjabi, S. Mehta, R. Chavan, V. Chitalia, D. Deogharkar, S. Deshpande, Efficiency of biosynthesized silver and zinc nanoparticles against multi-drug resistant pathogens, Front. Microbiol. 9 (2018) 2207.
[20] G. Kampf, Biocidal agents used for disinfection can enhance antibiotic resistance in gram-negative species, Antibiotics 7 (4) (2018).

[21] G. Mi, D. Shi, M. Wang, T.J. Webster, Reducing bacterial infections and biofilm formation using nanoparticles and nanostructured antibacterial surfaces, Adv. Healthc. Mater. 7 (13) (2018) 1–23.

[22] J.A. Lemire, J.J. Harrison, R.J. Turner, Antimicrobial activity of metals: mechanisms, molecular targets and applications, Nat. Rev. Microbiol. 11 (6) (2013) 371–384.

[23] C. Greulich, D. Braun, A. Peetsch, J. Diendorf, B. Siebers, M. Epple, M. Köller, The toxic effect of silver ions and silver nanoparticles towards bacteria and human cells occurs in the same concentration range, RSC Adv. 2 (17) (2012) 6981.

[24] A.L. Kubo, I. Capjak, I.V. Vrček, O.M. Bondarenko, I. Kurvet, H. Vija, A. Ivask, K. Kasemets, A. Kahru, Antimicrobial potency of differently coated 10 and 50 nm silver nanoparticles against clinically relevant bacteria Escherichia coli and Staphylococcus aureus, Colloids Surf., B 170 (2018) 401–410.

[25] A.L. Flores-Mireles, J.N. Walker, M. Caparon, S.J. Hultgren, Urinary tract infections: epidemiology, mechanisms of infection and treatment options, Nat. Rev. Microbiol. 13 (5) (2015) 269–284.

[26] N. Sabir, A. Ikram, G. Zaman, L. Satti, A. Gardezi, A. Ahmed, P. Ahmed, Bacterial biofilm-based catheter-associated urinary tract infections: causative pathogens and antibiotic resistance, Am. J. Infect. Control 45 (10) (2017) 1101–1105.

[27] D.P. Linklater, V.A. Baulin, S. Juodkazis, R.J. Crawford, P. Stoodley, E.P. Ivanova, Mechano-bactericidal actions of nanostructured surfaces, Nat. Rev. Microbiol. 19 (1) (2021) 8–22.

[28] V.B. Damodaran, N.S. Murthy, Bio-inspired strategies for designing antifouling biomaterials, Biomater. Res. 20 (1) (2016) 18.

[29] G.S. Watson, D.W. Green, J.A. Watson, Z. Zhou, X. Li, G.S.P. Cheung, M. Gellender, A simple model for binding and rupture of bacterial cells on nanopillar surfaces, Adv. Mater. Interfac. 6 (10) (2019) 1–8.

[30] D.P. Linklater, S. Juodkazis, E.P. Ivanova, Nanofabrication of mechano-bactericidal surfaces, Nanoscale 9 (43) (2017) 16564–16585.

[31] A. Elbourne, J. Chapman, A. Gelmi, D. Cozzolino, R.J. Crawford, V.K. Truong, Bacterial-nanostructure interactions: the role of cell elasticity and adhesion forces, J. Colloid Interface Sci. 546 (2019) 192–210.

[32] R. Texidó, S. Borrós, Allylamine PECVD modification of PDMS as simple method to obtain conductive flexible polypyrrole thin films, Polymers 11 (12) (2019) 2108.

[33] Chinga Gary, Johnsen Per Olav, Robert Dougherty, Elisabeth Lunden Berli, Quantification of the 3D microstructure of SC surfaces, J. Microsc. 227 (2007) 254–265.

[34] S. Hohmann, A. Neidig, B. Kühl, F. Kirschhöfer, J. Overhage, G. Brenner-Weiß, A new data processing routine facilitating the identification of surface adhered proteins from bacterial conditioning films via QCM-D/MALDI-ToF/MS, Anal. Bioanal. Chem. 409 (25) (2017) 5965–5974.

[35] R.A. Welch, V. Burland, G. Plunkett, P. Redford, P. Roesch, D. Rasko, E.L. Buckles, S.R. Liou, A. Boutin, J. Hackett, et al., Extensive mosaic structure revealed by the complete genome sequence of uropathogenic Escherichia coli, Proc. Natl. Acad. Sci. USA 99 (26) (2002) 17020–17024.

[36] K.D. Mandakhalikar, J.N. Rahmat, E. Chiong, K.G. Neoh, L. Shen, P.A. Tambyah, Extraction and quantification of biofilm bacteria: method optimized for urinary catheters, Nat. Sci. Reports 8 (1) (2018) 1–9.

[37] A. Mas-Vinyals, J. Gilabert-Porres, L. Figueras-Esteve, S. Borrós, Improving linking interface between collagen-based hydrogels and bone-like substrates, Colloids Surf., B 181 (2019) 864–871.

[38] D. Horna, J.C. Ramírez, A. Cifuentes, A. Bernad, S. Borrós, M.a. González, Efficient cell reprogramming using bioengineered surfaces, Adv. Healthc. Mater. 1 (2) (2012) 177–182.

[39] A. Cifuentes, S. Borrós, Comparison of two different plasma surface-modification techniques for the covalent immobilization of protein monolayers, Langmuir 29 (22) (2013) 6645–6651.

[40] D.H.K. Nguyen, V.T.H. Pham, V.K. Truong, I. Sbarski, J. Wang, A. Balčytis, S. Juodkazis, D.E. Mainwaring, R.J. Crawford, E.P. Ivanova, Role of topological scale in the differential fouling of: Pseudomonas aeruginosa and Staphylococcus aureus bacterial cells on wrinkled gold-coated polystyrene surfaces, Nanoscale 10 (11) (2018) 5089–5096.

[41] Z. Xiaoxue, W. Ling, L. Erkki, Superhydrophobic surfaces for the reduction of bacterial adhesion, RSC Adv. 3 (2013) 12003–12020.

[42] K. Anselme, P. Davidson, A.M. Popa, M. Giazzon, M. Liley, L. Ploux, The interaction of cells and bacteria with surfaces structured at the nanometre scale, Acta Biomater. 6 (10) (2010) 3824–3846.

[43] A. Marmur, From hygrophilic to superhygrophobic: theoretical conditions for making high-contact-angle surfaces from low-contact-angle materials, Langmuir 24 (14) (2008) 7573–7579.

[44] W.K. Lee, W. Bin Jung, S.R. Nagel, T.W. Odom, Stretchable superhydrophobicity from monolithic, three-dimensional hierarchical wrinkles, Nano Lett. 16 (6) (2016) 3774–3779.

[45] P. Roach, N.J.J. Shirtcliffe, M.I.I. Newton, Progess in superhydrophobic surface development, Soft Matter 4 (2) (2008) 224–240.

[46] C. García-Bonillo, R. Texidó, G. Reyes-Carmenaty, J. Gilabert-Porres, S. Borrós, Study of the human albumin role in the formation of a bacterial biofilm on urinary devices using QCM-D, ACS Appl. Bio Mater. 3 (5) (2020) 3354–3364.

[47] V.B. Damodaran, N.S. Murthy, Bio-inspired strategies for designing antifouling biomaterials, Biomater. Res. 20 (1) (2016) 18.

[48] L. Montero, S.H. Baxamusa, S. Borros, K.K. Gleason, L. Montero, S.H. Baxamusa, S. Borros, K.K. Gleason, Thin hydrogel films with nanoconfined surface reactivity by photoinitiated chemical vapor deposition thin hydrogel films with nanoconfined surface reactivity by photoinitiated chemical vapor deposition 26, 2009, pp. 399–403.

[49] M. Artigues, J. Gilabert-Porres, R. Texidó, S. Borrós, J. Abellà, S. Colominas, Analytical parameters of a novel glucose biosensor based on grafted pfm as a covalent immobilization technique, Sensors 21 (12) (2021) 1–15.

[50] K.K.S. Lau, K.K. Gleason, Particle surface design using an all-dry encapsulation method, Adv. Mater. 18 (15) (2006) 1972–1977.

[51] W.K. Jung, H.C. Koo, K.W. Kim, S. Shin, S.H. Kim, Y.H. Park, K.J. Woo, C.K. Hye, W.K. Ki, S. Shin, et al., Antibacterial activity and mechanism of action of the silver ion in Staphylococcus aureus and Escherichia coli, Appl. Environ. Microbiol. 74 (7) (2008) 2171–2178.

[52] A.B.G. Lansdown, Silver in health care: antimicrobial effects and safety in use interactions between skin and biofunctional metals, Curr Probl Dermatol. Basel, Karger 33 (2006) 17–34.

[53] B. Kharisov, O. Kharissova, U. Ortiz-Mendez, CRC Concise Encyclopedia of Nanotechnology, 2016.

[54] E.C. Hagan, M.S. Donnenberg, H.L.T. Mobley, Uropathogenic Escherichia Coli, EcoSal Plus 3 (2) (2009).

[55] M.E. Terlizzi, G. Gribaudo, M.E. Maffei, UroPathogenic Escherichia coli (UPEC) infections: virulence factors, bladder responses, antibiotic, and non-antibiotic antimicrobial strategies, Front. Microbiol. 8 (2017).

[56] E.P. Ivanova, J. Hasan, H.K. Webb, G. Gervinskas, S. Juodkazis, V.K. Truong, A.H.F. Wu, R.N. Lamb, V.A. Baulin, G.S. Watson, et al., Bactericidal activity of black silicon, Nat. Commun. 4 (2013) 1–7.

[57] E.M. Hetrick, M.H. Schoenfisch, Reducing implant-related infections: active release strategies, Chem. Soc. Rev. 35 (9) (2006) 780–789.